

# A deviatoric softening law for predicting the deformation of soft clays subject to anisotropic consolidation

Cong Shi & Jinyuan Liu

Department of Civil Engineering - Ryerson University, Toronto, Canada

Tareq Salloum

Ontario Power Generation, Niagara-on-the-Lake, Canada

Laifa Cao

WSP Global Inc, Ontario, Canada



## ABSTRACT

The well-known Modified Cam-Clay (MCC) family of models employ an isotropic hardening law, where the size change of yield locus is governed only by plastic volumetric strain increment or decrement. However, reviewing the incremental anisotropic consolidation tests performed on soft clays at various stress ratios reveals the presence of deviatoric softening (DS). The anisotropic consolidation tests applied with higher stress ratios tend to result in higher compressibility of the investigated clays. This indicates that the deviatoric strain can cause the yield surface to contract. To address this issue, the volumetric hardening law has been modified to incorporate soil softening owing to plastic deviatoric strain increment. This new DS law is easy to implement and requires only one additional parameter to govern the yield surface contraction. The new DS model has incorporated this DS law into the rotational anisotropic hardening law of S-CLAY1. The model has been verified through simulations of a number of incremental anisotropic consolidation tests collected from the literature. It is demonstrated that the modified softening law can provide an improved prediction of deformation of soft clays subject to the anisotropic consolidation tests under different stress ratios.

## RÉSUMÉ

Les modèles bien connus de la famille MCC (Modified Cam-Clay) utilisent une loi de durcissement isotrope, selon laquelle le changement de taille du locus de rendement est régi uniquement par l'augmentation ou la diminution progressive de la déformation volumétrique plastique. Cependant, l'examen des tests de consolidation anisotropes incrémentaux effectués sur des argiles molles sous différents rapports de contrainte révèle la présence d'un ramollissement déviatorique (DS). Les tests de consolidation anisotropique appliqués avec des rapports de contrainte plus élevés ont tendance à entraîner une compressibilité plus élevée des argiles étudiées. Cela indique que la déformation déviatorique provoquera la contraction de la surface de rendement. Pour remédier à ce problème, la loi de durcissement volumétrique a été modifiée pour intégrer le ramollissement des sols en raison de l'augmentation de la déformation plastique du déviateur. Cette nouvelle loi d'adoucissement déviatorique est facile à mettre en œuvre et ne nécessite qu'un paramètre supplémentaire pour régir la contraction de la surface de rendement. Le nouveau modèle DS a intégré cette loi DS à la loi de durcissement anisotrope par rotation de S-CLAY1. Le modèle a été vérifié au moyen de simulations d'un certain nombre de tests de consolidation anisotropes supplémentaires recueillis dans la littérature. Il est démontré que la loi de ramollissement modifiée peut fournir une meilleure prévision de la déformation des argiles molles soumises aux tests de consolidation anisotropique sous différents rapports de contrainte.

## 1. INTRODUCTION

Hardening and softening behavior of soil refers to the yield stress increase and decrease due to accumulated plastic strains. For example, yield surface will increase as the result of the incremental plastic volumetric strain, which is usually known as volumetric hardening (Roscoe and Burland 1968). Hardening and softening can also be understood as shear strength evolution when soil is subject to shearing stress, like during triaxial tests. This behavior, linking shear strains with shear strength evolution, is known as distortional hardening or softening (Zabala and Alonso 2011, Conte et al. 2013).

A pertinent example for volumetric hardening would be one-dimensional or isotropic compression tests

where yield stress increases due to increased loading. The soil fails in none of the two compression tests since the stress ratios in both cases are usually lower than the failure stress ratio. Stress ratio is defined as  $\eta = \frac{q}{p'}$ .  $p'$  is the mean effective stress defined as

$$p' = \frac{\sigma'_{xx} + \sigma'_{yy} + \sigma'_{zz}}{3} \quad [1]$$

where  $\sigma'_{xx}$ ,  $\sigma'_{yy}$  and  $\sigma'_{zz}$  are effective normal stresses at  $x$ ,  $y$ ,  $z$  directions respectively. The deviatoric stress  $q$  is defined to be

$$q = \left\{ \frac{1}{2} \left[ (\sigma'_{xx} - \sigma'_{yy})^2 + (\sigma'_{yy} - \sigma'_{zz})^2 + (\sigma'_{zz} - \sigma'_{xx})^2 \right] + 3(\tau_{yz}^2 + \tau_{zx}^2 + \tau_{xy}^2) \right\}^{\frac{1}{2}} \quad [2]$$

where  $\tau_{xy}$ ,  $\tau_{xy}$  and  $\tau_{xy}$  are shear stresses.

It is usually assumed that the increase of yield stress is the result of yield surface expansion owing to predominantly plastic volumetric strain. Therefore, many chose to solely link plastic volumetric strain with yield surface expansion (Cam-Clay family) to constitute hardening laws in their models (Nakai and Matsuoka 1986, Liu and Carter 1999, Yao et al. 2008, Chen and Yang 2017) as shown below

$$dp'_m = \frac{vp'_m}{\lambda - \kappa} d\varepsilon_v^p \quad [3]$$

where  $p'_m$  is the size of the yield surface,  $v = 1 + e_0$  the specific volume.  $\lambda$  and  $\kappa$  are respectively the virgin compression index and recompression index defined in an isotropic stress space.  $d\varepsilon_v^p$  is the plastic volumetric strain increment.

Besides, one may also include plastic deviatoric strain in yield surface hardening laws, but the cases of models adopting this approach are less than that of ones with volumetric hardening models (Krenk 2000, Collins and Kelly 2002), known as biased volumetric hardening model. In these biased volumetric hardening models referred, both plastic deviatoric strain and plastic volumetric strain are assumed to contribute to the yield surface expansion.

However, the review of the incremental anisotropic consolidation tests (IAC) conducted on soft clays from the existing publications (Wiltafsky et al. 2002, Zentar et al. 2002, Wheeler et al. 2003, Karstunen and Koskinen 2008, Qualitas 2016) reveal that plastic deviatoric strain will cause yield surface to contract. During these tests, incremental loads were applied at daily intervals to soil samples while maintaining constant stress ratios constant. Multiple loading and unloading stages were considered in these tests. It is observed that loading stages applied at higher stress ratios cause a more compressible response of soil than those at lower stress ratios. For this reason, a modified deviatoric softening law has been proposed in this study to account for this behavior.

The modified softening law has been combined with the well-established anisotropic model S-CLAY1 to become a new model (DS). S-CLAY1 is a Cam-Clay like critical state model considering the rotation of yield surface and its evolution during loading. The details of S-CLAY1 will be discussed in section 3.2. The prediction of this new model (DS) in this paper has been compared with modified Cam Clay (MCC) and S-CLAY1, to demonstrate its capability in simulating anisotropy consolidation tests.

## 2. EXPERIMENTAL RESULTS OF INCREMENTAL ANISOTROPIC CONSOLIDATION TESTS ON REMODED MURRO CLAY

Murro clay is a black silty clay found in western coast of Finland with clay-size fraction of 30%. The black color of Murro clay is due to the presence of sulfur. The water content of the soil is found to be between 65% to 100%. The plastic index  $I_p$  varies from 31 to 66. The typical

sensitivity is below 14 (Karstunen and Yin 2010). Some IAC tests results of remolded Murro clay can be found in Figure 1. Both tests shown here were published in (Karstunen and Koskinen 2008) and interpreted by the authors of this paper. The samples were fully remolded before finishing primary consolidation in a one-dimensional condition at a load of 15 kPa. Then, the samples were transferred into a triaxial cell to consolidate at a designed initial stress ratio  $\eta_0 = 0.65$  to reproduce the in situ state. After the initial consolidation was complete, the samples were unloaded at a low stress level close to 10 kPa before the incremental anisotropic consolidation was commenced.

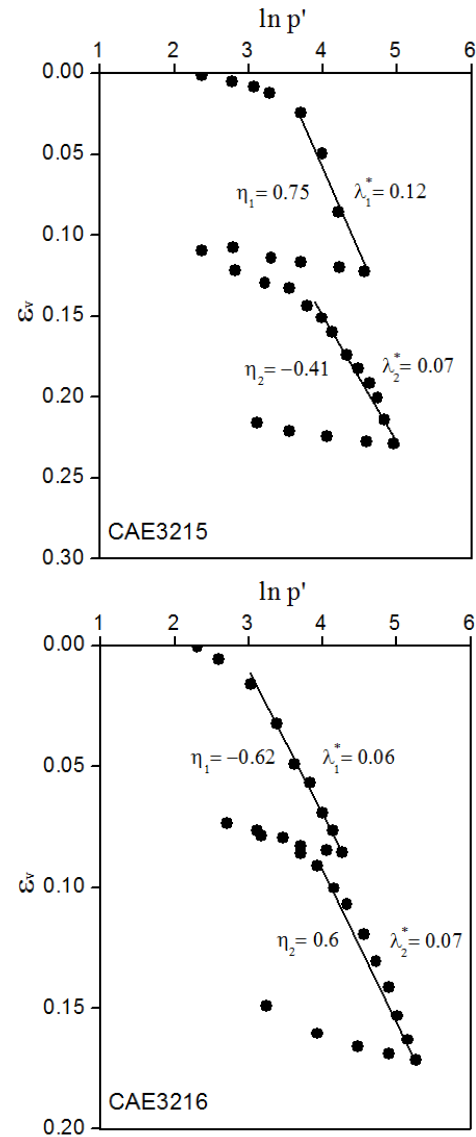


Figure 1. Results of incremental anisotropic consolidation tests on remolded Murro clay (Karstunen and Koskinen 2008)

Test CAE3215 in Figure 1 includes two loading stages. At the first stage, the sample was consolidated at a stress ratio of  $\eta_1 = 0.75$ , yielding the modified compressive index  $\lambda_1^* = 0.12$  from its linear normal consolidation line. The modified compressive index  $\lambda^* = \frac{\lambda}{1+e_0}$  is used here for normalization purpose considering void ratio difference of samples. Similarly, the volumetric strain  $\varepsilon_v = \frac{\Delta e}{1+e_0}$  is used instead of  $\Delta e$ . The first loading stage was followed by an unloading stage at the same stress ratio. Subsequently, the sample was extended at  $\eta_2 = -0.41$  at the second loading stage. The negative sign here indicates the applied confining pressure is higher than vertical pressure ( $q = \sigma'_y - \sigma'_x < 0$ ). A lower  $\lambda_2^* = 0.07$  has been yielded at this stage. It is understood that  $\eta_1 = 0.75$  which is of higher absolute value than  $\eta_2 = -0.41$  will induce more significant plastic deviatoric strain  $d\varepsilon_d^p$  as per the dilatancy law of MCC model:

$$\frac{d\varepsilon_d^p}{d\varepsilon_v^p} = \frac{2\eta}{M^2 - \eta^2} \quad [4]$$

Test CAE3216 has two loading stages with very similar stress ratios in absolute value ( $\eta_1 = -0.62, \eta_2 = 0.60$ ). Two stages of loading result in very close modified compressive index. The first loading stage yields an approximate  $\lambda_1^* = 0.06$ , slightly lower than the second stage  $\lambda_2^* = 0.07$ .

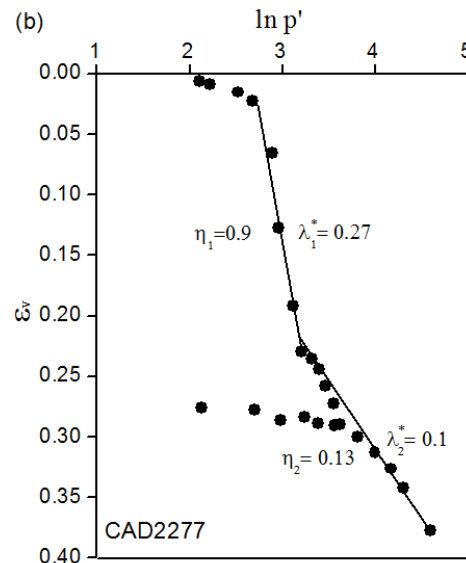
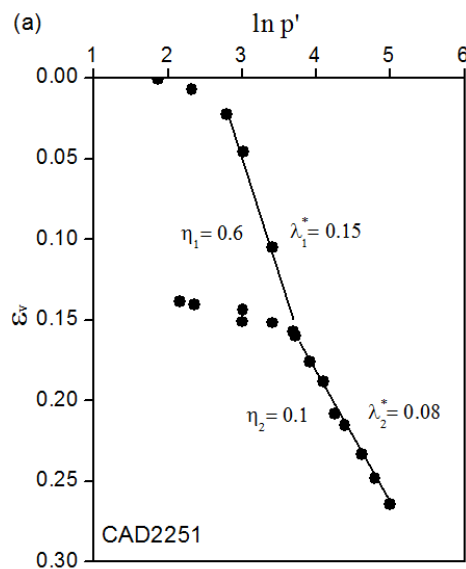
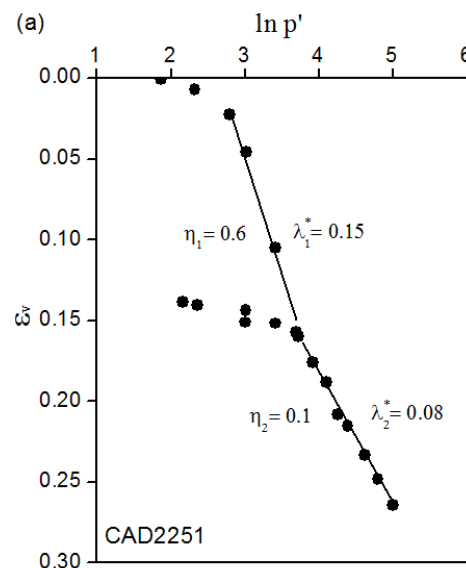


Figure 2. Results of incremental anisotropic consolidation tests on undisturbed Otaniemi clay (Wheeler et al. 2003)

Otaniemi clay is found in southern Finland at the shore of the Gulf of Finland. Otaniemi clay has a high clay-sized fraction of 78% and is mainly composed of illite. The Otaniemi clay was extracted undisturbed for the tests. The IAC tests on undisturbed Otaniemi clay are reported in (Wheeler et al. 2003). The results were digitized and plotted in Test CAE3216 has two loading stages with very similar stress ratios in absolute value ( $\eta_1 = -0.62, \eta_2 = 0.60$ ). Two stages of loading result in very close modified compressive index. The first loading stage yields an approximate  $\lambda_1^* = 0.06$ , slightly lower than the second stage  $\lambda_2^* = 0.07$ .



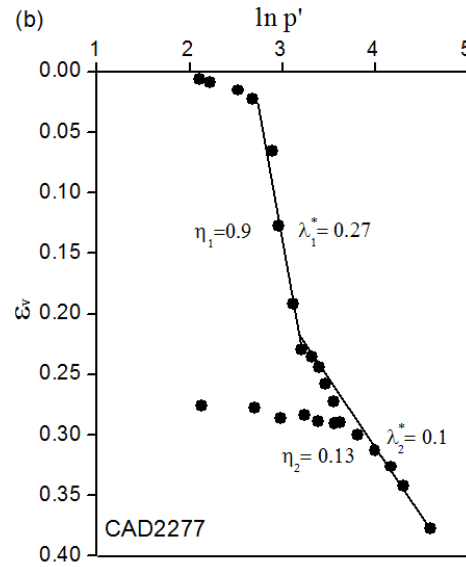
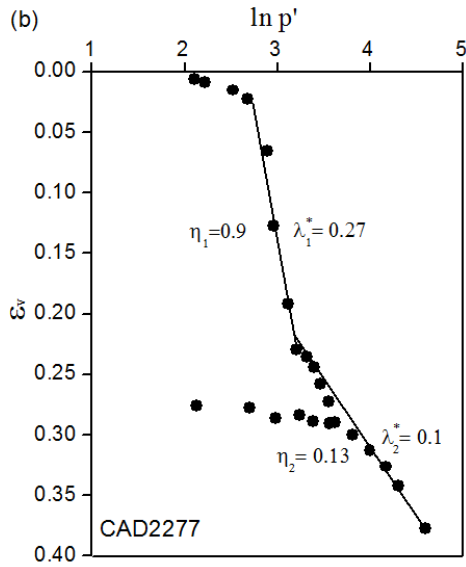


Figure 2. The Otaniemi clay samples were retrieved by Norwegian and Swedish piston sampler. The undisturbed sample has the natural water content more than 90%, and sensitivity of 7 to 14.

A small stress increment of 2-5 kPa was employed in the test to maintain a low excess pore pressure level, but this caused each test to take eight weeks to finish. As seen in Test CAE3216 has two loading stages with very similar stress ratios in absolute value ( $\eta_1 = -0.62, \eta_2 = 0.60$ ). Two stages of loading result in very close modified compressive index. The first loading stage yields an approximate  $\lambda_1^* = 0.06$ , slightly lower than the second stage  $\lambda_2^* = 0.07$ .

Figure 2, both CAD2251 and CAD 2277 tests involved two compression loading stages with distinct stress ratios. Both samples didn't show destructuration behavior since the obtained normal consolidation lines appeared to be linear. Test CAD2251 obtains a steeper compression slope of  $\lambda_1^* = 0.15$  from stage one loading applied at  $\eta_1 = 0.6$  than stage two ( $\lambda_2^* = 0.08, \eta_2 = 0.1$ ). Test CAD2277 applied a very high stress ratio of 0.9 at first loading stage, one close to the reported critical state ratio ( $M = 1.1$ ). The sample responded with a higher compressibility  $\lambda_1^* = 0.27$ , compared to the stage two ( $\lambda_2^* = 0.1$ ) which loaded the sample at a lower stress ratio  $\eta_2 = 0.1$ . Note that  $\lambda_1^* = 0.27$  in CAD2277 is also higher than  $\lambda_1^* = 0.15$  obtained the first stage in CAD2251 under the constant ratio of  $\eta_1 = 0.6$ .

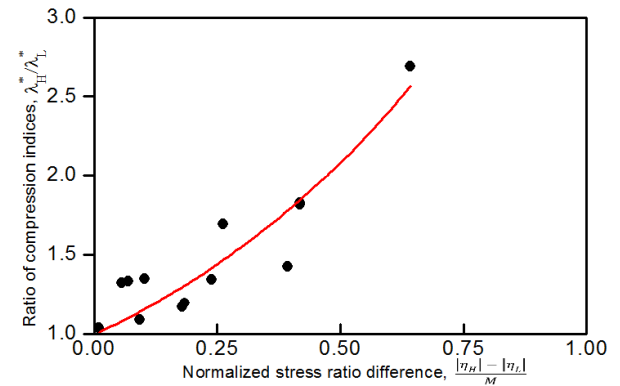
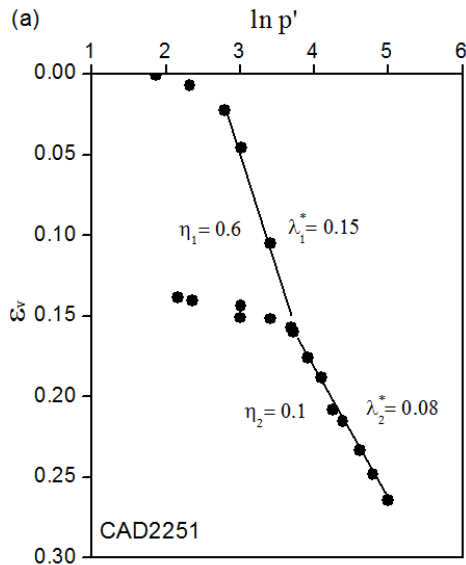


Figure 3. Variation between stress ratio difference and normalized compression index ratio from incremental anisotropic consolidation tests on soft soils

A total of 13 IAC tests involving two or multiple loading stages of different stress ratios have been digitized. As shown in Figure 3, the compression indices obtained within the same tests are normalized by the compression index of the second loading stage.  $\lambda_H^*/\lambda_L^*$ , which denotes the ratio between the higher and lower compression index of an IAC test. The results are plotted

against the normalized difference of corresponding stress ratios ( $(|\eta_H| - |\eta_L|)/M$ ).

The dependence of compression indices on stress ratios (stress paths) are demonstrated by the results. The soils consolidated under high stress ratios regardless of its sign, tend to exhibit increased compressibility. It is explained by the plastic deviatoric strain induced softening behavior, which causes yield surface to contract. A smaller yield surface makes the compression slope steeper at the same volumetric strain level. A higher stress ratio regardless of its sign generates a more deviatoric strain, as shown in Equation [4].

An exponential relationship between the stress ratio difference and normalized compression index ratio has been proposed:

$$\frac{\lambda_H^*}{\lambda_L^*} = e^{1.21|\eta_H - \eta_L|} \quad [5]$$

To predict the normalized isotropic compression index, here one can assign the lower stress ratio  $\eta_0 = 0$  and thus:

$$\lambda_0^* = \frac{\lambda_H^*}{e^{1.21|\eta_H|}} \quad [6]$$

where  $\lambda_0^*$  is the compression index corresponding to the isotropic consolidation ( $\eta_0 = 0$ ).

DS is similar to the destructuration that causes the structured surface to shrink. The experimental results as concluded in this paper, however, indicate the presence of deviatoric softening are also found in the soils not exhibiting strong destructuration behavior (reference to support your claim). One possible approach to simulate this behavior is to consider the deviatoric softening in the volumetric hardening law. This will be detailed in the subsequent section.

### 3. DESCRIPTION OF THE MODIFIED DEVIATORIC SOFTENING MODEL (DS)

#### 3.1 Modified deviatoric softening law

In light of the softening behavior noticed from the IAC tests on soft soil, the modification of the existing volumetric softening law is needed to account for stress ratio association with yield surface contraction.

In this work, the biased hardening law in (Krenk 2000, Collins and Kelly 2002, Liu et al. 2013) is modified to assume the plastic deviatoric strain's contribution to softening. This softening law is built within the framework of the volumetric hardening law:

$$dp'_m = \frac{vp'_m}{\lambda - \kappa} (d\varepsilon_v^p - \zeta \cdot \eta \cdot d\varepsilon_d^p) \quad [6]$$

where  $d\varepsilon_d^p$  is the plastic deviatoric strain increment.  $\zeta$  is the weighting factor that governs the deviatoric softening.

The DS law here assumes that stress ratio and its induced plastic deviatoric strain cause the yield surface to shrink. A weighting factor,  $\zeta$ , would be used to adjust the degree of softening, with a high value assigned to

amplify the softening. On the other side, the softening law retains the hardening of yield surface due to plastic volumetric strain increment. The model reduces to the volumetric hardening law when either of  $\zeta$  or  $\eta$  is assigned zero. The new softening law is now combined with the anisotropic model S-CLAY1, where the dilatancy law becomes

$$\frac{d\varepsilon_d^p}{d\varepsilon_v^p} = \frac{2(\eta - \alpha)}{M^2 - \eta^2} \quad [7]$$

where  $\alpha$  is the inclination of yield surface. Combine [6] with [7], one can obtain

$$dp'_m = \frac{vp'_m}{\lambda - \kappa} \frac{M^2 - \eta[\eta(1 - 2\zeta) + 2\alpha\zeta]}{M^2 - \eta^2} d\varepsilon_v^p \quad [8]$$

Assigning zero to  $\eta$  and  $\zeta$  reduces the hardening law to MCC volumetric hardening law

$$dp'_m = \frac{vp'_m}{\lambda - \kappa} d\varepsilon_v^p \quad [9]$$

The general stress and plastic strain relationship would be

$$\begin{bmatrix} d\varepsilon_v^p \\ d\varepsilon_q^p \end{bmatrix} = \frac{\lambda - \kappa}{vp'_m} \cdot \frac{M^2 - \eta^2}{M^2 - \eta[\eta(1 - 2\zeta) + 2\alpha\zeta]} \cdot \begin{bmatrix} M^2 - \eta^2 & 2\eta \\ 2\eta & 4\eta^2 \end{bmatrix} \cdot \begin{bmatrix} dp'_m \\ dq \end{bmatrix} \quad [10]$$

#### 3.2 Evolutional yield surface anisotropy

DS model employs an inclined Modified Cam-Clay (MCC) yield surface same as S-CLAY1 model to account for anisotropy:

$$f = g = (q - \alpha p')^2 - (M^2 - \alpha^2)(p'_m - p')p' = 0 \quad [11]$$

Assuming an associated flow, the yield surface rotation is governed by  $\alpha$  and the size is controlled by  $p'_m$ , see Figure 4.  $M_c$  denotes the critical state slope of compression case and  $M_e$  for extension case.

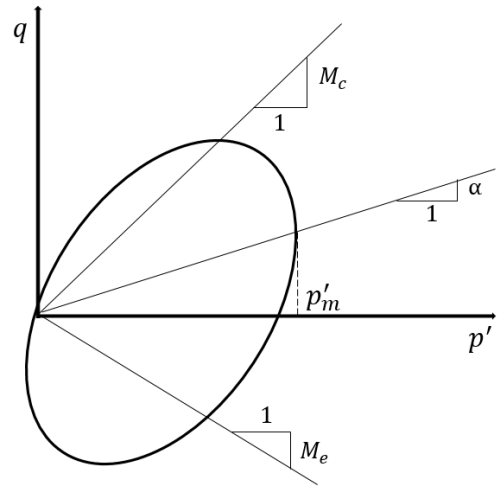


Figure 4. Inclined yield surface of S-CLAY1 model

Inclination  $\alpha$  dynamically approaches  $\frac{3}{4}\eta$  and  $\frac{\eta}{3}$  simultaneously during plastic straining, also controlled

by both plastic volumetric strain  $d\varepsilon_v^p$  and plastic deviatoric strain  $d\varepsilon_d^p$ .

$$d\alpha = \mu \left[ \left( \frac{3\eta}{4} - \alpha \right) \langle d\varepsilon_v^p \rangle + \beta \left( \frac{\eta}{3} - \alpha \right) |d\varepsilon_d^p| \right] \quad [12]$$

#### 4. MODEL VERIFICATION THROUGH ANISOTROPIC TRIAXIAL TESTS CONSIDERING DEVIATORIC SOFTENING

##### 4.1 Model description

In this section, a number of IAC tests will be modeled in Plaxis 2D with DS model to verify its capacity of reproducing deviatoric softening. The axisymmetric geometry of test samples with a radius of 2.5 cm and a height of 10.2 cm is assumed based on the standard 1:2 diameter height ratio. See Figure 5 for the details.

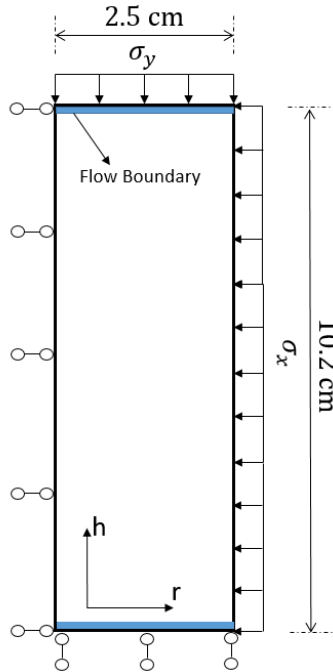


Figure 5. Axisymmetric sample geometry for test modeling in Plaxis 2D

The left boundary is fixed in horizontal direction and the vertical displacement is fixed at bottom boundary. Drainage is allowed at right boundary and both top and bottom boundaries. The target loading of each unloading-reloading stage is in consistence with the simulated tests. The geometry is discretized into a typical total of 208 axisymmetric triangular elements. This number of elements or more is found to result in consistent model predictions.

##### 4.2 Parameters input of DS model

The model verification is conducted by simulating three IAC tests on Finnish clay. The model predictions have been compared with S-CLAY1 and MCC simulation results published in (Wheeler et al. 2003, Karstunen and Koskinen 2008). Since these tests were previously modeled using S-CLAY1 and MCC, most of model parameters can be thus conveniently determined (Table 1), such as the saturated unit weight  $\gamma$ , the size of yield surface  $p'_m$ , the permeability  $k$ , the coefficient of earth pressure at rest  $K_0$ , the Poisson's ratio, the initial void ratio  $e_0$ . Anisotropic parameter inputs for the modeling are also the same as the literature, including the initial yield surface inclination  $\alpha_0$ , the absolute rate of yield surface rotation  $\mu$  and the relative rate of yield surface rotation  $\beta$ .

Table 1. Values for the initial state parameters used in the test modeling

Test No.	Soil type	Disturbance	$\gamma$ kN/m <sup>3</sup>	$p'_m$ kPa	$k$ $\times 10^{-4}$ m/d	$K_0$	$\nu$	$e_0$	$t_0$ day	$\alpha_0$	$\mu$	$\beta$	$M_c$	$M_e/M_c$
CAD2277	Otaniemi	Undisturbed	16	18	1.0	0.67	0.3	2.86	1	0.42	20	0.50	1.1	0.73
CAE2544	Otaniemi	Undisturbed	16	22	1.0	0.67	0.3	3.79	1	0.30	20	0.67	1.1	0.73
CAE3215	Murro	Remolded	16	35.5	1.0	0.67	0.2	1.99	1	0.46	20	0.67	1.6	0.65

DS model employs  $\lambda_0$  that should be obtained from isotropic consolidation tests. The value of  $\lambda_0$  (isotropic case), were back calculated from [3]. Recall that  $\lambda_0 = \lambda^*(1 + e_0)$ . It should be noted that for S-CLAY1 and MCC model,  $\lambda$  and  $\kappa$  are probably from the fitting of the  $\varepsilon_v \sim \ln p'$  of the second loading stage. The  $M_e/M_c$  ratio is estimated using

$$\frac{M_e}{M_c} = \frac{3 - \sin \varphi_c}{3 + \sin \varphi_c} \quad [13]$$

where  $M_e$  is the critical state stress ratio on the extension slide.  $\sin \varphi_c$  is the critical stage frictional angle defined as

$$\sin \varphi_c = \frac{3M_c}{6 + M_c} \quad [14]$$

Table 2. Parameters for deviatoric softening modeling

Test No.	$\lambda_0$	$\kappa$	$\zeta$
----------	-------------	----------	---------

CAD2277	0.33	0.04	7
CAE2544	0.22	0.04	6
CAE3215	0.13	0.03	15

Table 3. Compression parameters for S-CLAY1 and MCC

Test No.	$\lambda$	$\kappa$
CAD2277	0.44	0.04
CAE2544	0.44	0.04
CAE3215	0.21	0.03

#### 4.3 Simulation of the tests on undisturbed Otaniemi clay and remolded Murro clay

Figure 6-9 present the simulation results of CAD2277 and CAE 2544 (undisturbed Otaniemi clay), and CAE3215 (remolded Murro clay) using DS model. The model prediction is compared with those of S-CLAY1 and MCC model. See CAD 2277 in Figure 6a, S-CLAY1 and MCC model are shown to be able to predict the volumetric strain  $\varepsilon_v$  development during the second loading stage by assigning an appropriate  $\lambda$  to both models, but this results in a significant underestimation of the volumetric strain of the first loading stage. In contrast, since the deviatoric softening is considered, DS is shown to well capture the volumetric strains at both stages. S-CLAY1 still provides a better estimation of yield stress than MCC due to the consideration of yield surface rotation. Moreover, DS has shown an improved overall prediction of the deviatoric strain  $\varepsilon_d$  in Figure 6b, as well as  $\varepsilon_d/\varepsilon_v$  ratio. However, MCC's prediction of  $\varepsilon_d$  is very deviant from the measurements. S-CLAY1's prediction of  $\varepsilon_d$  is much more acceptable than MCC, albeit some underestimation exists.

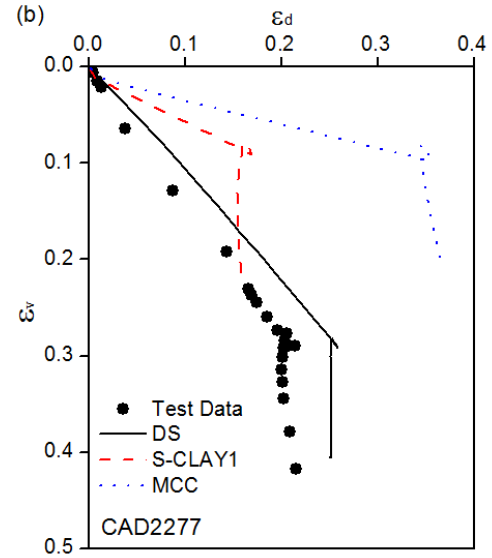
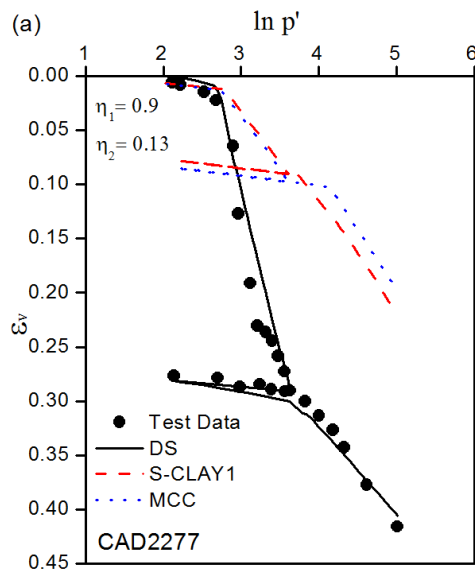
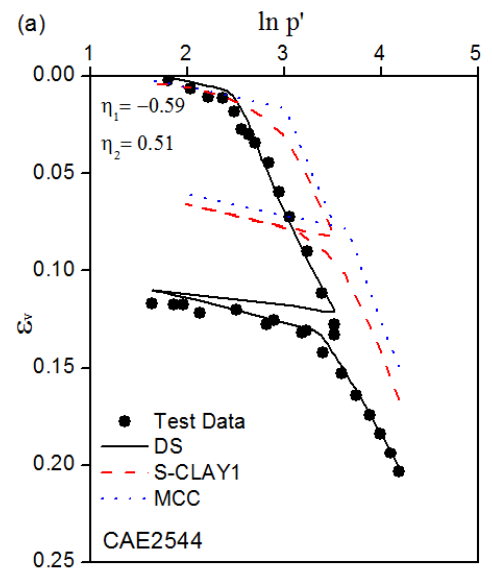


Figure 6. Model simulation of CAD2277:(a)  $\varepsilon_v \sim \ln p'$ , (b)  $\varepsilon_d \sim \varepsilon_v$ .

For the test CAE2544 (Figure 7), the volumetric strain is still under-predicted by S-CLAY1 and MCC, whereas DS well predicts  $\varepsilon_v$  for both loading stages. It is shown that both DS and S-CLAY1 can better capture the yield stresses than MCC, which again tends to over-predict the value (Figure 7a). The yield stress predicted by S-CLAY1 at the first stage is difficult to identify from the rounded reloading transition. This is due to the rapid yield surface rotation from the initial positive value towards negative (Wheeler et al. 2003). This issue is mitigated by DS by considering deviatoric softening that results in a steeper slope. Both DS and S-CLAY1 model provide an adequately accurate approximation of  $\varepsilon_d \sim \varepsilon_v$  path for both loading stages, as seen in **Error! Reference source not found.** MCC again overestimates  $\varepsilon_d$ .



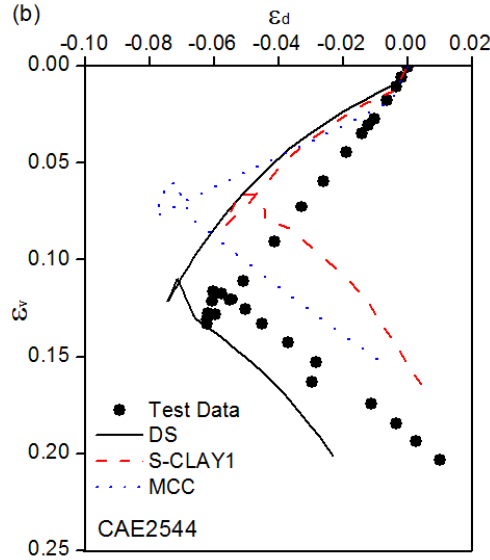


Figure 7. Model simulation of CAE2544: (a)  $\varepsilon_v \sim \ln p'$ , (b)  $\varepsilon_d \sim \varepsilon_v$ .

Figure 8 presents the model simulation of test CAE3215, which involves the first loading stage as triaxial compression ( $\eta_1 = 0.75$ ) and the second stage as triaxial extension ( $\eta_2 = -0.41$ ), as shown in Figure 8a. All three models employed in this study appear to adequately capture the yield stress at the first loading stage, but MCC still slightly over-predicts the yield stress. DS is shown to provide a more accurate volumetric strain prediction than S-CLAY1 and MCC. However, all three models seem to over-predict the yield stress at the second loading stage, which causes the underestimation of  $\varepsilon_v$ . For the  $\varepsilon_d \sim \varepsilon_v$  path prediction shown in Figure 8b, both DS and S-CLAY1 predict  $\varepsilon_d$  reasonably well during the first loading stage, in contrast to MCC. For the second loading stage, S-CLAY1 and MCC appear to better capture the  $\varepsilon_d \sim \varepsilon_v$  path than DS.

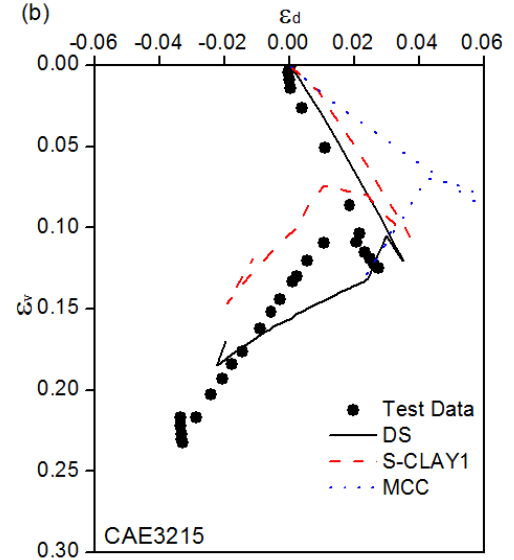
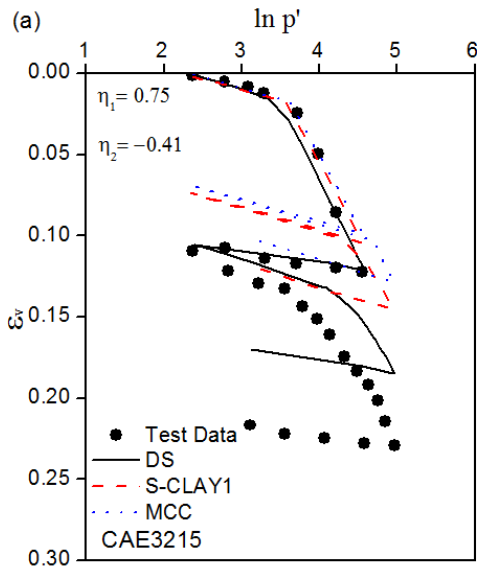


Figure 8. Model simulation of CAE3215: (a)  $\varepsilon_v \sim \ln p'$ , (b)  $\varepsilon_d \sim \varepsilon_v$ .

## 5. DISCUSSION AND CONCLUSION

This study proposes a modified deviatoric softening law, which considers the soil compressibility's dependence on stress ratios when conducting anisotropic consolidation tests. This simple softening law assumes the plastic deviatoric strain to contribute to yield surface contraction. A new soil model named DS has incorporated this softening law, and has been combined with S-CLAY1 model to account for yield surface anisotropy. The verification of DS has been conducted through the simulation of a number of incremental anisotropic consolidation tests. The predictions of soil deformation by DS model are compared with S-CLAY1 and MCC predictions. The main conclusions of this paper are listed as follows:

1. The literature review of a number of incremental anisotropic consolidation tests indicates that soft soils manifest a more compressible response when consolidated at a higher stress ratio.
2. The modified deviatoric softening law requires only one additional parameter  $\zeta$ , to govern the contribution of the plastic deviatoric strain to the yield surface contraction.
3. The modified deviatoric softening law can be reduced to the volumetric hardening law employed by S-CLAY1 and MCC, if a soil is under isotropic consolidation or  $\zeta$  is assigned as zero.
4. Simulation of anisotropic consolidation tests demonstrates that DS model provides improvement prediction of soil compressibility under various stress ratios, as well as deviatoric strains.

However, limitations of this modified softening model exist due to its mathematical assumptions.

1. Model prediction of strains becomes sensitive to  $\zeta$  at high stress ratios. This would result in a less accurate prediction in plastic strains when the soil is consolidated at the ratios close to the critical state ratio  $M$ . For this reason, the use of this model should be applied with caution when simulating the high stress ratio cases.
2. The natural variation of different types of clay leads to the scattering of  $\frac{\lambda_H}{\lambda_L}$  and  $\frac{|\eta_H| - |\eta_L|}{M}$  dependence seen in Figure 3. Therefore, Equation [6] can lead to erroneous estimation of  $\lambda_0$ , which adversely affect strain prediction of the model.

## 6. ACKNOWLEDGEMENT

The authors want to extend gratitude to Dr. Yin Jian-Hua from The Hong Kong Polytechnic University for sharing the model codes containing S-CLAY1 model, and Chinese Scholarship Council for providing the financial support.

## 7. REFERENCE

- Chen, Y.N., and Yang, Z.X. 2017. A family of improved yield surfaces and their application in modeling of isotropically over-consolidated clays. *Computers and Geotechnics*, **90**(August 2018): 133–143. Elsevier Ltd. doi:10.1016/j.compgeo.2017.06.007.
- Collins, I.F., and Kelly, P.A. 2002. A thermomechanical analysis of a family of soil models. *Géotechnique*, **52**(7): 507–518. doi:10.1680/geot.2002.52.7.507.
- Conte, E., Donato, A., and Troncone, A. 2013. Progressive failure analysis of shallow foundations on soils with strain-softening behaviour. *Computers and Geotechnics*, **54**: 117–124. Elsevier Ltd. doi:10.1016/j.compgeo.2013.07.002.
- Karstunen, M., and Koskinen, M. 2008. Plastic Anisotropy of Soft Reconstituted Clays. *Canadian Geotechnical Journal*, **45**(3): 314–328. doi:10.1139/T07-073.
- Karstunen, M., and Yin, Z.Y. 2010. Modelling time-dependent behaviour of Murro test embankment. *Geotechnique*, **60**(10): 735–749. doi:10.1680/geot.8.P.027.
- Krenk, S. 2000. Characteristic state plasticity for granular materials Part I: Basic theory. *International Journal of Solids and Structures*, **37**(43): 6343–6360. doi:10.1016/S0020-7683(99)00278-4.
- Liu, M.D., and Carter, J.P. 1999. Virgin compression of structured soils. *Géotechnique*, **49**(1): 43–57. doi:10.1680/geot.1999.49.1.43.
- Liu, W., Shi, M., Miao, L., Xu, L., and Zhang, D. 2013. Constitutive modeling of the destructuration and anisotropy of natural soft clay. *Computers and Geotechnics*, **51**: 24–41. Elsevier Ltd. doi:10.1016/j.compgeo.2013.01.011.
- Nakai, T., and Matsuoka, H. 1986. A generalized elastoplastic constitutive model for clay in three-dimensional stresses. *Soils and Foundations*, **26**(3): 81–89. doi:10.1061/ASCE1090-02412003129:112.
- Qualitas. 2016. Internal Report, Waba Dam Investigation Arnprior, Ontario.
- Roscoe, K.H., and Burland, J.B. 1968. On the generalized stress-strain behavior of “wet” clay. *Engineering Plasticity*,: 535–609. doi:10.1016/0022-4898(70)90160-6.
- Wheeler, S.J., Anu, N., Karstunen, M., and Matti. 2003. An anisotropic elastic-viscoplastic model for soft clays. *Canadian Geotechnical Journal*, **40**: 403–418. doi:10.1016/j.jgsolstr.2009.11.004.
- Wiltafsky, C., Messerklinger, S., and Schweiger, H.F. 2002. An advanced multilaminate model for clay. *In Proceedings of the 8th International Symposium on Numerical Models in Geomechanics-NUMOG VIII, Rome, Italy.* pp. 67–73.
- Yao, Y.P., Sun, D.A., and Matsuoka, H. 2008. A unified constitutive model for both clay and sand with hardening parameter independent on stress path. *Computers and Geotechnics*, **35**(2): 210–222. doi:10.1016/j.compgeo.2007.04.003.
- Zabala, F., and Alonso, E.E. 2011. Progressive failure of Aznalcóllar dam using the material point method. *Géotechnique*, **61**(9): 795–808. doi:10.1680/geot.9.P.134.
- Zentar, R., Karstunen, M., Wiltafsky, C., Schweiger, H.F., and Koskinen, M. 2002. Comparison of two approaches for modelling anisotropy of soft clays. *In Proceedings of the 8th International Symposium on Numerical Models in Geomechanics-NUMOG VIII, Rome, Italy.* pp. 115–121.